ELECTROSPINNING OPTIMIZATION FOR FABRICATION OF FLEXIBLE TRANSPARENT ELECTRODES

An Undergraduate Research Scholars Thesis

by

MEGAN DAWKINS

Submitted to the Undergraduate Research Scholars program at
Texas A&M University
in partial fulfillment of the requirements for the designation as an

UNDERGRADUATE RESEARCH SCHOLAR

Approved by Research Advisor: Dr. Ying Li

May 2019

Major: Mechanical Engineering

TABLE OF CONTENTS

Page

ABSTRACT 1

DEDICATION 2

ACKNOWLEDGEMENTS 3

NOMENCLATURE 4

LIST OF FIGURES 5

CHAPTER

I. INTRODUCTION 7

II. METHODS 10

Overview 10
Electrospinning 10
Optimization of Electrospinning Solution 12
Optimization of Electrospinning Processes 14
Scanning Electron Microscopy 15
Sputtering 17

III. RESULTS 19

IV. CONCLUSION 25

REFERENCES 27

ABSTRACT

Electrospinning Optimization for Fabrication of Flexible Transparent Electrodes

Megan Dawkins
Department of Mechanical Engineering
Texas A&M University

Research Advisor: Dr. Ying Li
Department of Mechanical Engineering
Texas A&M University

Flexible, transparent electrodes (FTEs) can be used in many applications, such as wearable electronics, flexible touch screens, and semitransparent solar cells [1]–[4]. Researchers have successfully created stretchable, bendable, and uniformly high-performing transparent electrodes using metal nanotroughs [3], metal nanowires with protective coatings [1], [4]–[6], and hybrid structures of graphene-gold nanotrough networks [2]. Although each of these methods utilizes electrospinning to create the nanonetwork, the procedures and desired characteristics of the electrospun fibers vary greatly from method to method.

The most widely established high-performing FTEs have been created by utilizing nanotrough networks [2], [3]. Some researchers found the best conductivity and transmissivity utilizing copper to make up these nanotroughs [3], but due to its instability when exposed to air, high temperatures, and humidity, others established more stable electrodes through use of more expensive metals such as gold or silver [2]. It is hypothesized that lower-cost, stable FTEs could be created utilizing copper nanotroughs sandwiched between protective atomic layers of metal oxides. Therefore, this research identifies, varies, and optimizes electrospinning parameters for the fabrication of such electrodes.

DEDICATION

This work is dedicated to my sister Hannah, who is one of the most incredible people I know.

ACKNOWLEDGEMENTS

I would like to thank Dr. Ying Li, my advisor, for challenging the way I think and inspiring me to work hard in my research endeavors. Great thanks go to Dr. Chao Li, the post-doctorate fellow who has mentored me, guided me, and taught me everything I know about research. I would also like to thank Xuhui Feng for making time to help me with sputtering and SEM, Yuwei Zhang for helping me with sputtering, and all of the graduate students in my lab who have offered their advice and aid throughout the whole of my project.

I could not have enjoyed this experience as thoroughly without the support of my great friends at A&M, the professors who have inspired in me an excitement for learning, and my parents, who never stop believing in me. My main acknowledgement is to God, the Creator of all that is, ever was, and ever shall be. The beauty of His creation is my motivation to explore the unknown through science.

NOMENCLATURE

ALD	Atomic Layer Deposition
FTE	Flexible Transparent Electrode
ITO	Indium Tin Oxide
LiCl	Lithium Chloride (powder)
PVA	Polyvinyl Alcohol (powder)
PVP	Polyvinylpyrrolidone (powder)
SEM	Scanning Electron Microscopy

LIST OF FIGURES

Figure 1. The fabrication and transfer process for nanotrough networks is depicted by Hui Wu et al. in Nature Nanotechnology [3]... 8

Figure 2. Electrospinning process [32]. 11

Figure 3. Electrospinning setup (collector depicted above is preliminary). 11

Figure 4. The PVA, LiCl, and PVP used in solution optimization were each in powder form.... 12

Figure 5. Electrospinning solution utilized throughout research. 13

Figure 6. Square-hole collector of thickness 0.005 in. 15

Figure 7. Scanning Electron Microscope (SEM). 16

Figure 8. Sputtering Diagram [36]. 17

Figure 9. Sputtering Machine. 18

Figure 10. Optimized Electrospinning Setup 19

Figure 11. SEM image of PVP fibers electrospun across circular frame collector shows non-uniform directions of fibers and non-uniform spaces between fibers.............................. 20

Figure 12. SEM Image of Electrospun PVP fibers shows that fiber diameters are significantly less than 1 μm. 21

Figure 13. SEM Image of Electrospun PVP fibers shows that fiber diameter is 330 nm............ 21

Figure 14. PVP fibers electrospun using optimized settings are randomly ordered. 22

Figure 15. Diameters of PVP fibers electrospun using optimized settings vary from 600 nm to 3 μm with an average diameter of 1.54 μm. 22

Figure 16. Spaces between PVP fibers electrospun using optimized settings are 4393 μm^2 on average. 23

Figure 17. When the diameter of the electrospinning needle is too large, coagulations of polymer solution cause inconsistencies in fiber diameters and network characteristics................. 23

Figure 18. Coagulations of polymer solution can decrease uniformity in network, decrease transparency, and decrease conductance.. 24

Figure 19. Optimized electrospun nanofiber network samples. 26

CHAPTER I

INTRODUCTION

Transparent electrodes are an essential component of many optoelectronic devices, including touch screens, interactive electronics, and building-integrated semitransparent photovoltaics. The application of flexible transparent electrodes to wearable technology could lead to innovations in popular and medical devices that would have previously been impossible.

The traditional thin films of indium tin oxide (ITO) that are used as transparent electrodes are expensive, brittle, have low infrared transmittance, and are limited by a low-abundance of indium [1]–[4]. Percolating networks of carbon nanotubes have been studied as a more flexible alternative to transparent conducting oxides [1], [7]–[10], but are limited by an inverse relationship between conductivity and transmissivity. To achieve lower resistance, thickness must be increased, which greatly decreases light transmittance [1], [3]. Another flexible alternative to indium tin oxide and other transparent conducting oxides is graphene [11]–[15], however these carbon-based electrodes face the same conductance-transmittance limitations as carbon nanotubes. To address the low conductance of carbon and polymer-based materials, strong, flexible metal nanowire networks have been studied, with sheet resistances of less than 10 Ω/sq. at 90% transmission achieved [1], [3], [16]–[23]. These metal nanowire networks must be designed or treated to be defect-free, have limited wire-to-wire junctions, and exhibit small junction resistance. Additionally, nanowire networks made from metals such as copper, which are unstable when exposed to air, high temperatures, and humidity, must be protected from the elements using further processes such as polymer protection layers, metal oxide protection layers, or graphene or nickel protective shells that increase cost, sheet resistance, and decrease transmittance [5], [6], [24]–[27]. Researchers have discovered that the conductivity of these bare electrodes can be preserved while the transmissivity and flexibility are improved by creating metal nanotroughs instead of metal nanowires [2], [3]. Nanotroughs are created by electrospinning water-soluble polymer fibers across an open substrate to create a free-standing polymer nanowire network. Small amounts of metal or metal-hybrids are then deposited onto one side of the fibers using forms of chemical or physical vapor deposition, such as sputtering. The metal-coated fibers are laminated onto a substrate, and finally the polymers are dissolved using an aqueous solution, leaving only trough-shaped metal fibers, as seen in Figure 1 [2], [3].

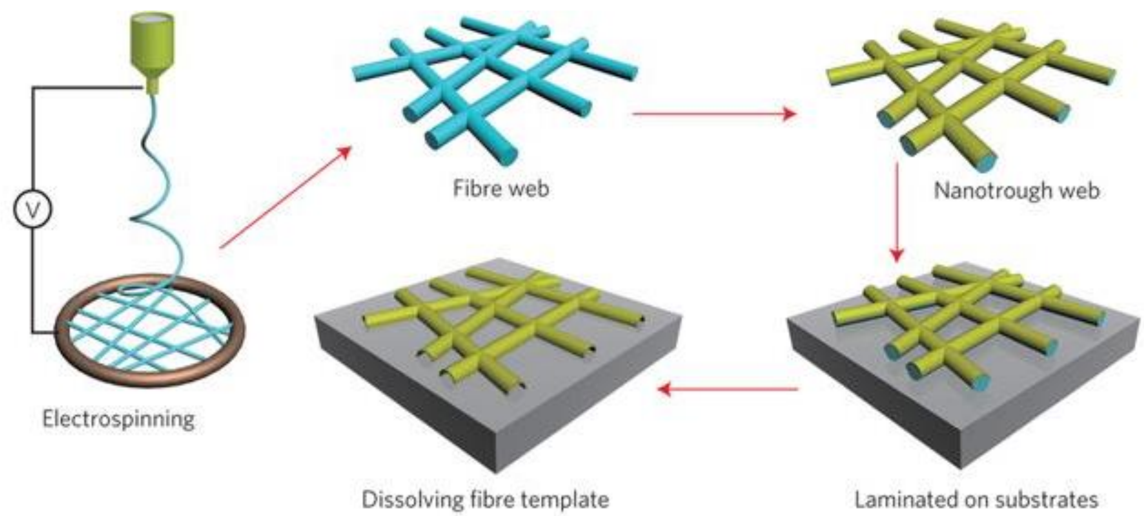

Figure 1. The fabrication and transfer process for nanotrough networks is depicted by Hui Wu et al. in Nature Nanotechnology [3].

The concave shape of the nanotroughs reduces the electromagnetic cross-section, which allows more visible light to pass through the spaces between the nanofibers [3]. Copper nanotrough networks have demonstrated remarkable performance of only 2 Ω/sq. resistance at 90% transmittance and 17 Ω/sq. resistance at 95% transmittance [3]. Unfortunately, copper nanotrough networks face many of the same challenges as copper nanowire networks due to the unstable nature of copper in response to air, high temperatures, and humidity. A possible solution to these issues are hybrid structures of graphene-metal nanotrough networks [2]. The graphene hybrid can increase conductive uniformity throughout the electrode without significantly reducing transmittance. Graphene also acts as a passivation layer, slowing the permeation of gas and moisture, and as a heat sink, spreading and dissipating heat [2], [28], [29]. These hybrids have demonstrated sheet resistances as low as 1.1 Ω/sq. at 91% transmittance, which is significantly better performance than FTEs fabricated from other methods. Unfortunately, this performance is achieved using gold, a metal which is on average 6000 times more expensive than copper [30]. In order to maintain high optoelectronic performance at lower fabrication costs, it is hypothesized that copper nanotrough networks could be coated in protective layers of light-colored metal oxides using atomic layer deposition. With only atoms of metal oxide separating the copper electrode from its substrate, it is expected that sheet resistance would not be significantly affected, and due to the reflective properties of light colors, transmittance is expected to be matched or exceeded with the addition of the protective layers. The purpose of this research is to determine the optimal electrospinning techniques and parameters for the fabrication of such FTEs.

CHAPTER II

METHODS

Overview

Using Dr. Ying Li's labs, metal nanotrough networks were created by electro-spinning water-soluble polyvinylpyrrolidone (PVP) polymers and then sputtering copper onto the electro-spun membrane. Next, the copper-polymer membrane was soaked in a solution to dissolve the polymer membrane, leaving a copper nanotrough network. The nanotrough network was then coated in a metal oxide to protect the metal from humidity and extreme environments. The type and thickness of the metal oxide was varied to determine the optimal protective layer for the electrode. The transmittance and sheet resistance were tested between each step of the process.

Electrospinning

Electrospinning is a highly adaptable, relatively low-cost method for making ultrafine fibers using a high-voltage power supply. To start, a syringe is filled with a polymer solution and its needle pointed towards a highly conductive collector. The syringe is slowly dispensed while a high voltage is run between the needle and the collector. Once the electric field reaches a critical value at which the repulsive electric force overcomes the surface tension of the polymer solution at the tip of the needle, the polymer solution is ejected from the needle tip to a collector. While traveling to the collector, the solution jet whips in a spiral motion and solidifies due to the fast evaporation of the solvent. It is deposited on the collector, resulting in a network of fibers ranging in diameter from hundreds of nanometers to several micrometers depending on user-defined system parameters, with arrangements formed according to the type of collector chosen [31]. A diagram of this process is depicted in Figure 2.

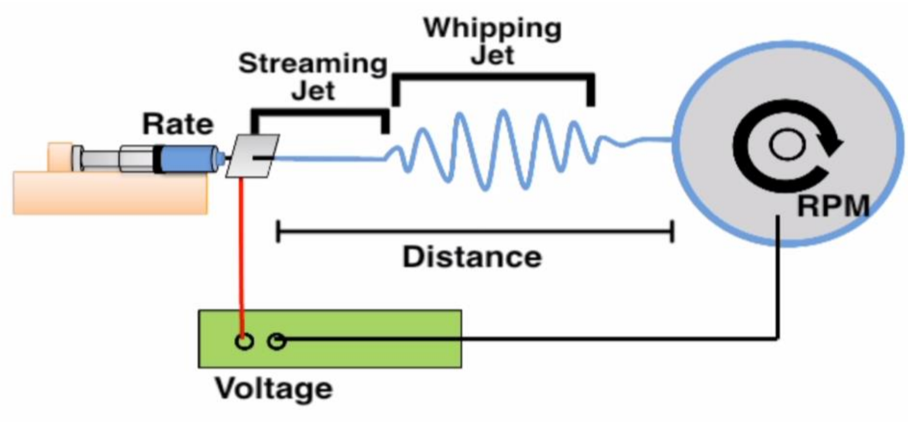

Figure 2. Electrospinning process [32].

The electrospinning machine used for this research was a Spellman SL60. The general setup for electrospinning used for this research is shown in Figure 3.

Figure 3. Electrospinning setup (collector depicted above is preliminary).

Optimization of Electrospinning Solution

The electrospinning solution was optimized using varied combinations of polyvinyl alcohol (PVA), polyvinylpyrrolidone (PVP), water, ethanol, and lithium chloride (LiCl). Further information on these chemicals and polymers is given in Figure 4.

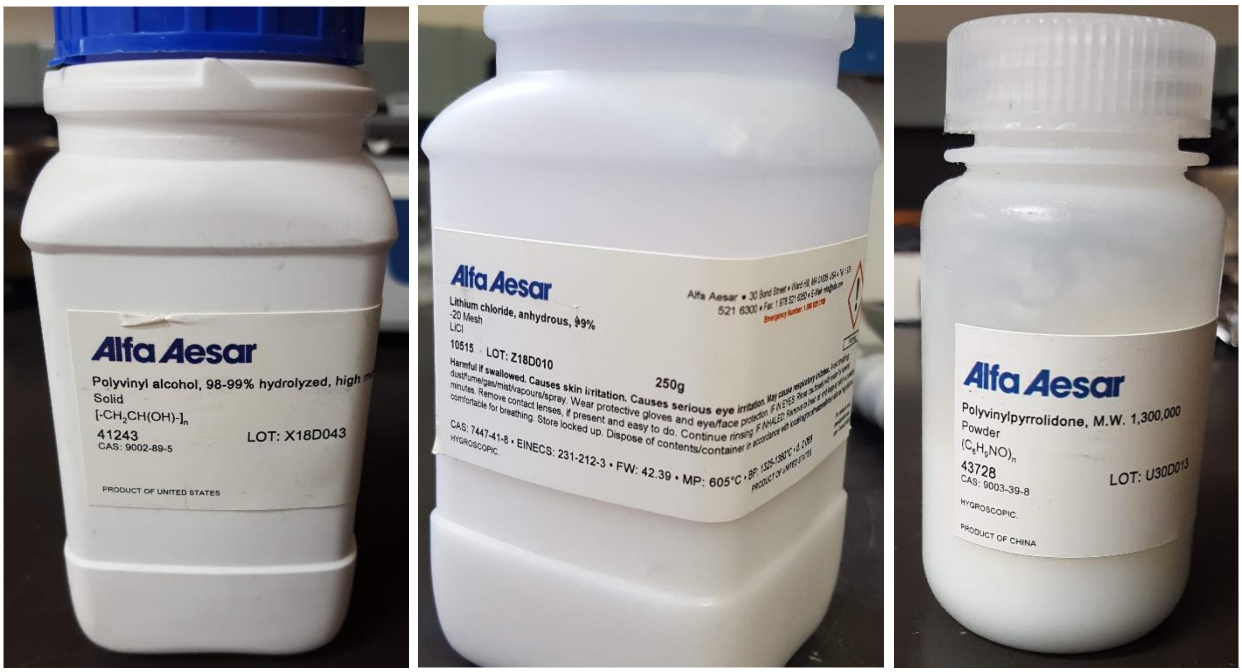

Figure 4. The PVA, LiCl, and PVP used in solution optimization were each in powder form.

The first parameter to vary was the choice of polymer. Other researchers found that between PVA and PVP, the optimal polymer for preparing copper nanotroughs was PVA [3]. The surface energy of polymer largely determines the metal coating quality, so the ideal polymer template must be identified. Following the results of this past research, the first solutions prepared were made by adding 90 wt.% (36 mL) deionized water to 10 wt.% (4 grams) PVA and stirring at 300 rpm, 125°C for 45 minutes. To increase conductivity of the polymer for electrospinning, 0.0008 grams of LiCl were added to future solutions. The weight percentages of

PVA, LiCl, water, and ethanol (used in conjunction with or as a substitute for water as a solvent) were varied to optimize this solution for electrospinning. Next the same variations were performed in optimizing a solution with PVP. Finally, it was determined that the most stable, predictable, and optimal properties of fibers could be electrospun using a solution of 8 wt.% PVP to 92 wt.% solvent, where the solvent was composed of 90 wt.% ethanol and 10 wt.% deionized water. This solution, as seen in Figure 5, was used to prepare all samples throughout this research.

Figure 5. Electrospinning solution utilized throughout research.

Optimization of Electrospinning Processes

Many parameters affect the flexibility, transmissivity, and conductivity of the final electrode. The ideal nanofiber network has thick fibers (~1.8μm), large gaps between fibers, and the fibers are randomly aligned so that the properties of the nanofiber network are consistent throughout [2]. The first parameter to be varied in the optimization of the process was fiber alignment. There are many ways to collect electrospun fibers, so the first method was to collect the fibers on a flat plate. Fibers collected on plates are somewhat randomly aligned. This can be favorable for flexible, transparent electrodes because if fibers are all aligned in the same direction, the fiber network loses strength in other directions. In applications where strength is only needed in one direction (uniaxial stress), or two directions (biaxial stress) it may be favorable for all fibers to be uniformly aligned, in which case a different type of collector should be used. Knowing this, the fibers first collected on a flat sheet collector had favorable arrangement. Once they were pulled up with forceps and placed on a substrate, they were also revealed to have thick, durable networks. Unfortunately, this made dissolving of the polymers difficult later in the fabrication process. Therefore the next types of collectors used were frames, resulting in free-standing fibers.

Square frames, rectangular frames, and circular frames, all of varying dimensions and made from varying materials (types of plastics and copper) were used to collect the fibers, resulting in various densities of fiber networks and various arrangements of fibers. A difficulty throughout the collector-varying process was that the collector needed to be able to be put into a sputtering machine. The first collectors were raised off of the flat plate so that no fibers would land on the plate between the edges of the frame. However, the collectors needed to be no more than 0.01 inches thick with exact dimensions and particular cutouts for screws in order to be used in the sputtering machine. There were many iterations of collectors before a solution was found to this concern. One of the failed attempts is shown in Figure 6.

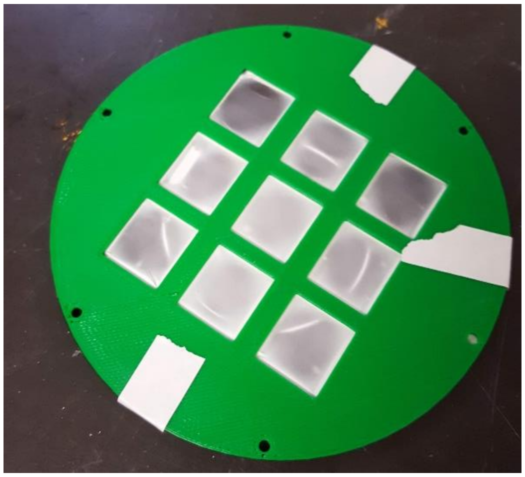

Figure 6. Square-hole collector of thickness 0.005 in.

Once the optimal shape and size of collector was determined, the electrospinning settings were varied. The first parameter to be optimized was the distance from the needle tip to collector. Then the voltage at which the electrospinning machine was operated, the volumetric flow rate of the polymer solution, the needle diameter, and the time spent electrospinning were varied in conjunction with each other because each of these parameters affect the diameter of the fibers. To adapt settings according to the results of the system (coagulation at needle tip, wet fibers, multiple jet streams, etc.) guides set forth by ElectrospinTech were referenced [33].

Scanning Electron Microscopy

Due to the nanoscale of the fiber networks, Scanning Electron Microscopy (SEM) was used to measure fibers. A scanning electron microscope (SEM) scans a focused electron beam over a surface to create an image. The electrons in the beam interact with the electrons in the sample, producing various signals that can be used to obtain information about the surface topography and composition [34]. For this particular testing, a JEOL JSM-7500F was utilized, as pictured in Figure 7.

Figure 7. Scanning Electron Microscope (SEM).

Sputtering

Sputtering is a form of Physical Vapor Deposition in which a vacuum process is used to deposit very thin films onto a substrate for a wide variety of commercial and scientific purposes. It occurs when an ionized gas molecule displaces atoms of a specific material. These atoms then bond at the atomic level to a substrate and create a thin film, as shown in Figure 8 [35].

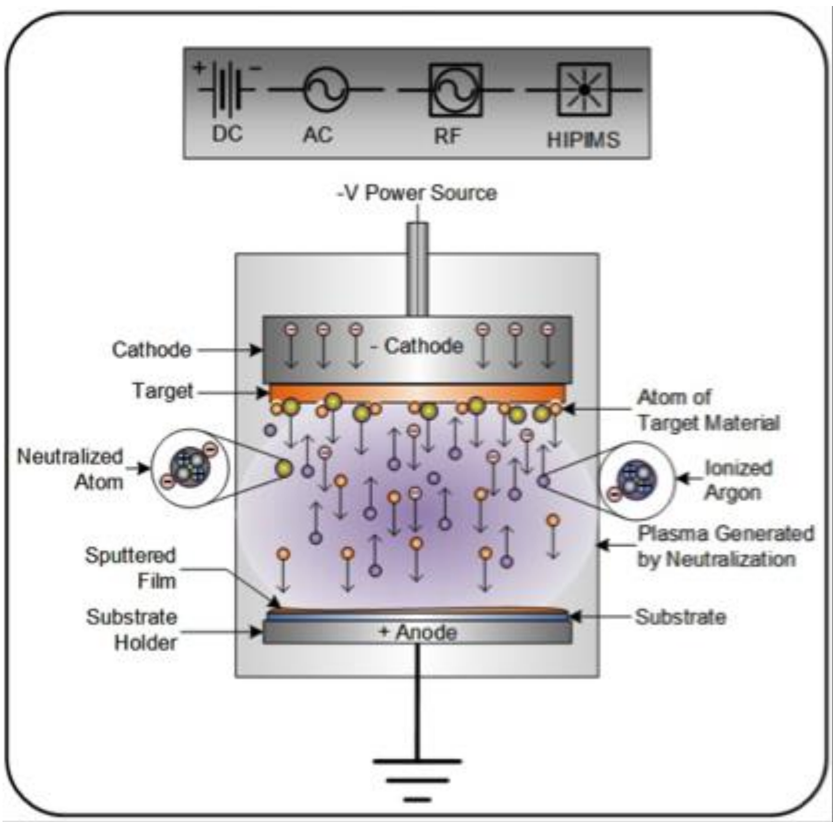

Figure 8. Sputtering Diagram [36].

For this research, 5 nm of gold was sputtered onto the fibers in order to use the Scanning Electron Microscope and 80 nm of copper was sputtered onto the fibers for testing of application to FTE fabrication. Samples are being sputtered in Figure 9.

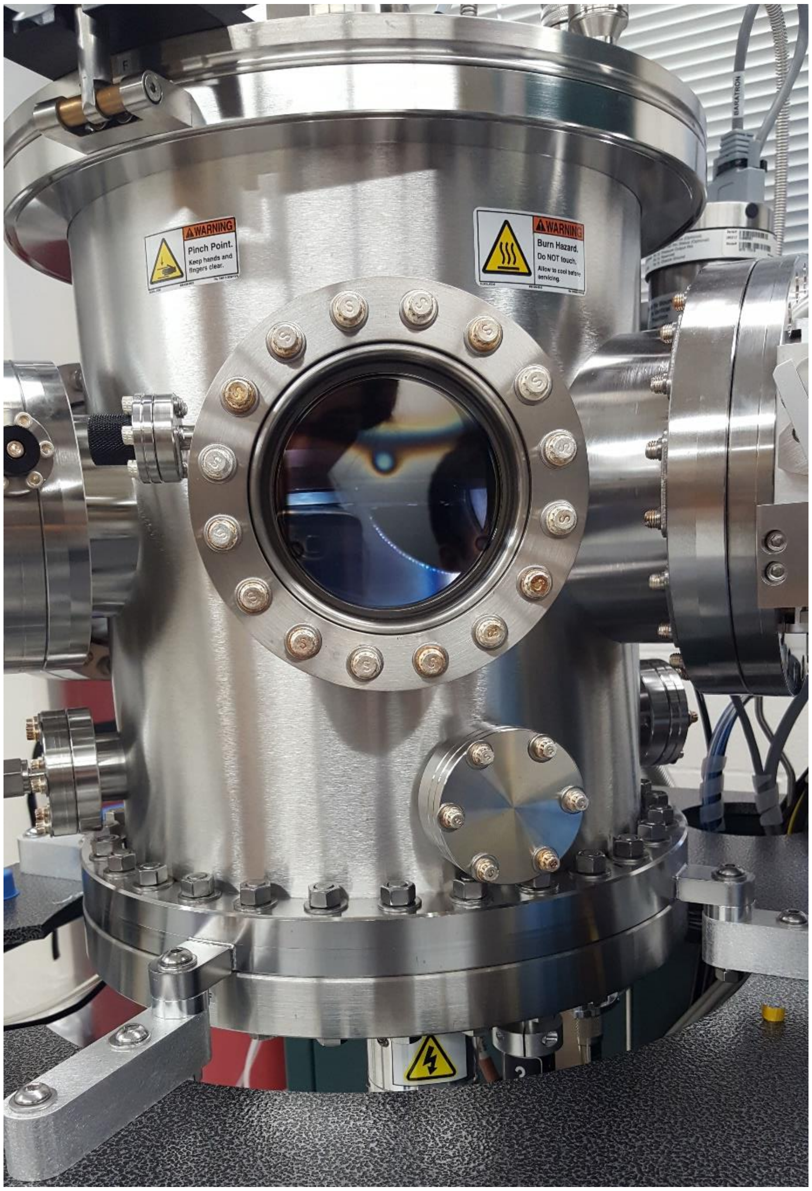

Figure 9. Sputtering Machine.

CHAPTER III

RESULTS

It was determined that the optimal electrospinning procedure for this research is to collect fibers across a metal circular frame collector 10 cm from the tip of the solution needle. The solution is pushed from the syringe at 0.6 μL/min, while 10 kV is run between the needle and the collector. The optimal needle is 30 mm long, with a 0.6 mm diameter (23G). To facilitate sputtering, a 1-inch long copper pipe of 0.75-inch inner diameter is placed on a flat plate so that the collection site on the end of the copper pipe is located 10 cm from the tip of the solution needle. See Figure 10 for setup.

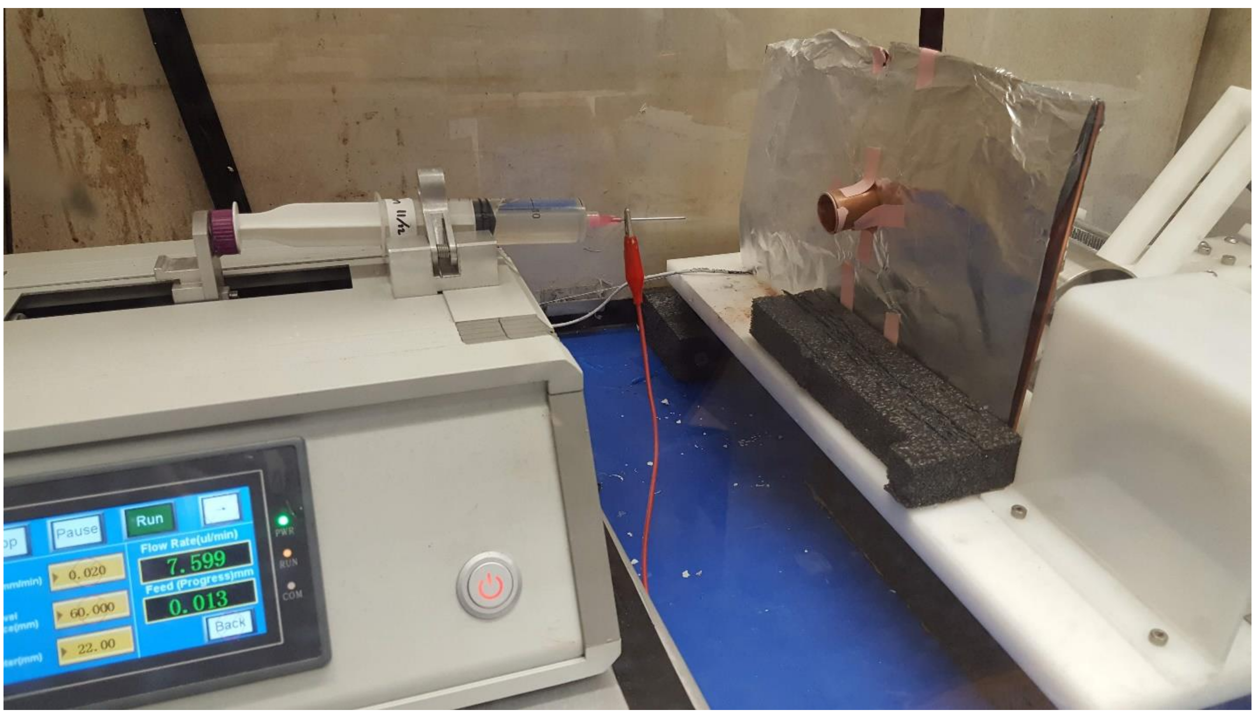

Figure 10. Optimized Electrospinning Setup

In order to come to these conclusions, nanofiber network characteristics had to be determined at each step in varying electrospinning parameters. Figures 11 thru 18 demonstrate results from varying samples. Properties of networks made from optimized electrospinning settings are noted in captions.

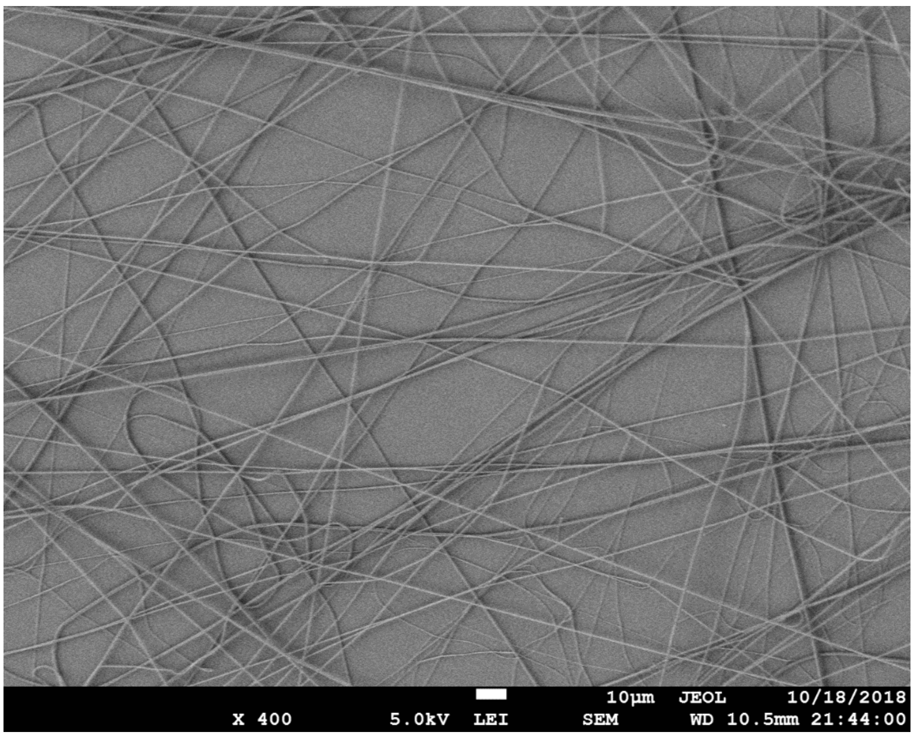

Figure 11. SEM image of PVP fibers electrospun across circular frame collector shows non-uniform directions of fibers and non-uniform spaces between fibers.

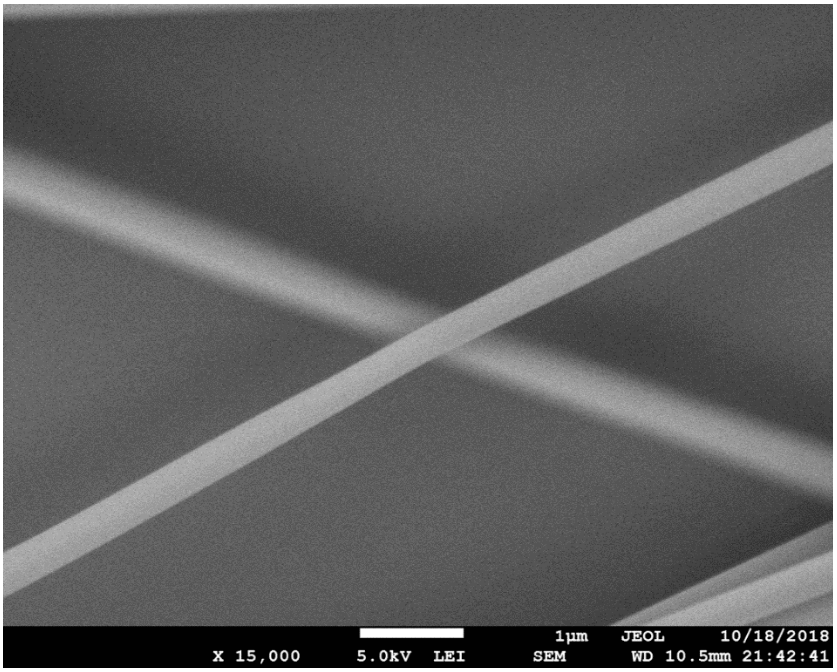

Figure 12. SEM Image of Electrospun PVP fibers shows that fiber diameters are significantly less than 1 μm.

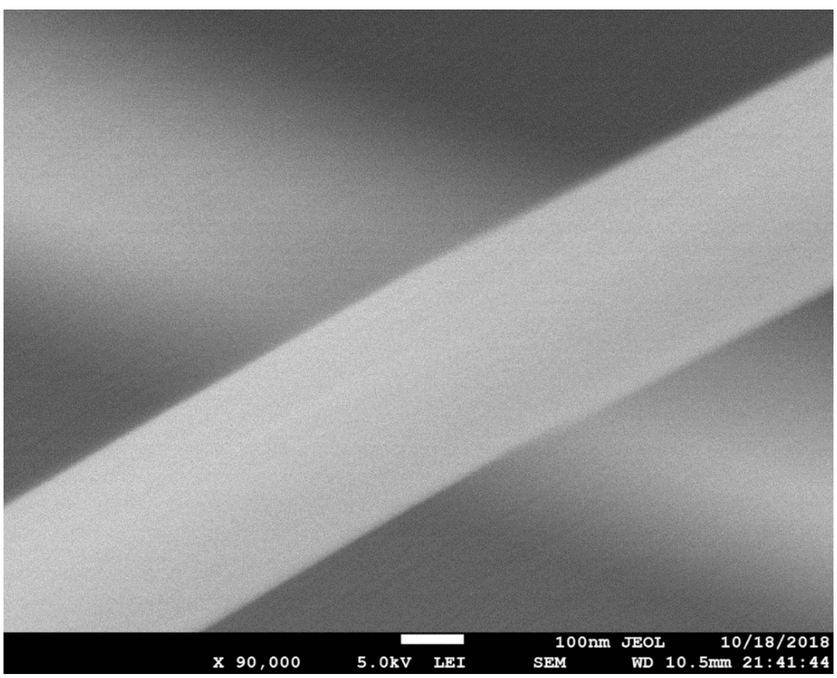

Figure 13. SEM Image of Electrospun PVP fibers shows that fiber diameter is 330 nm.

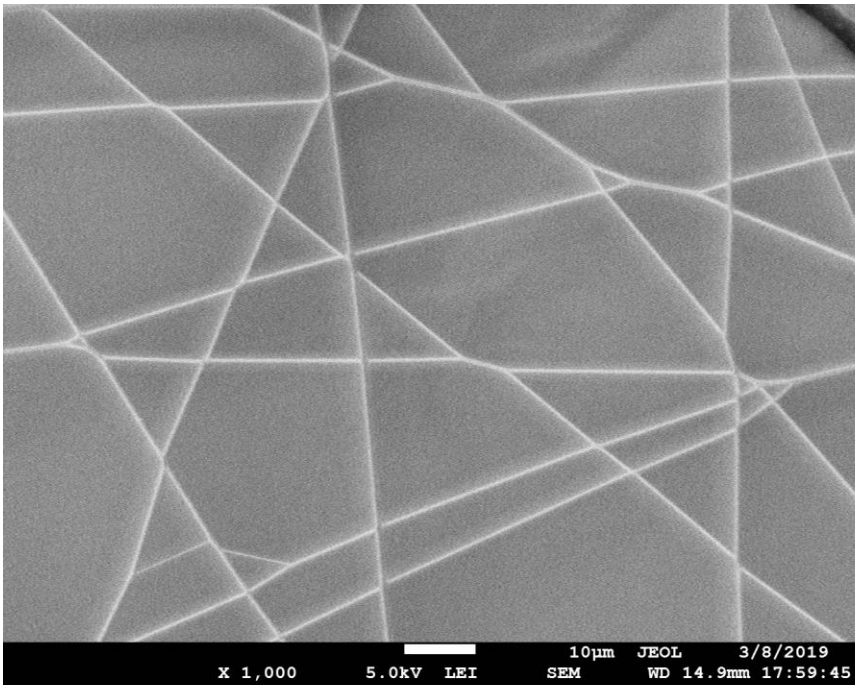

Figure 14. PVP fibers electrospun using optimized settings are randomly ordered.

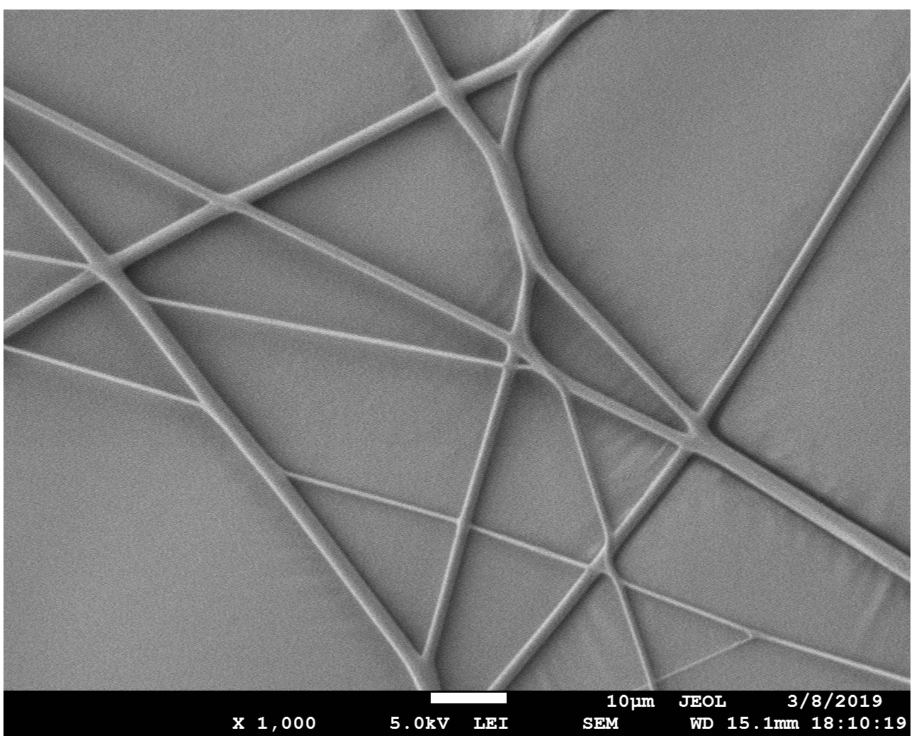

Figure 15. Diameters of PVP fibers electrospun using optimized settings vary from 600 nm to 3 µm with an average diameter of 1.54 µm.

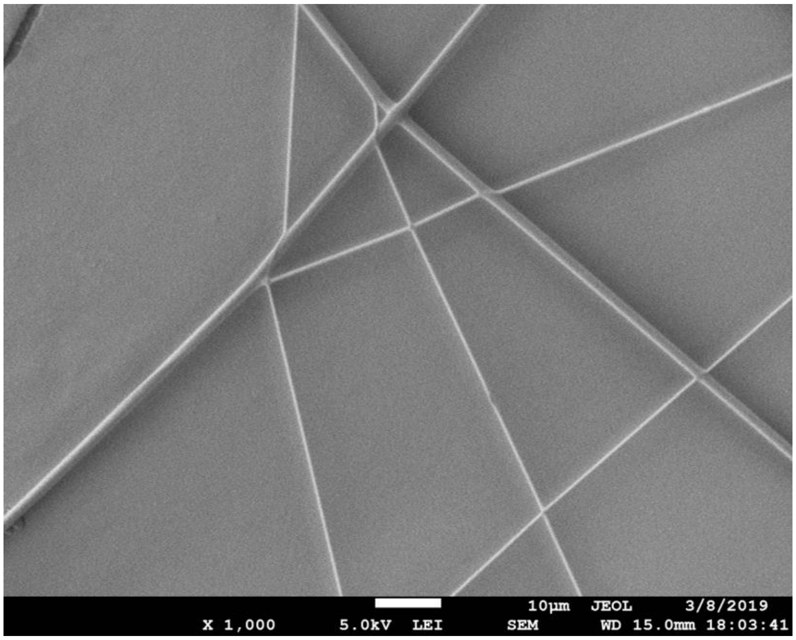

Figure 16. Spaces between PVP fibers electrospun using optimized settings are 4393 μm^2 on average.

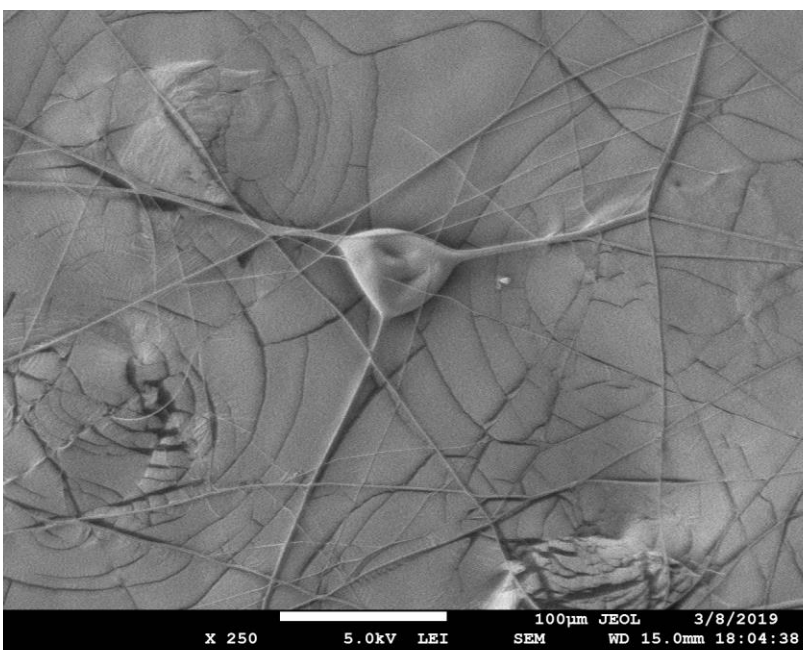

Figure 17. When the diameter of the electrospinning needle is too large, coagulations of polymer solution cause inconsistencies in fiber diameters and network characteristics.

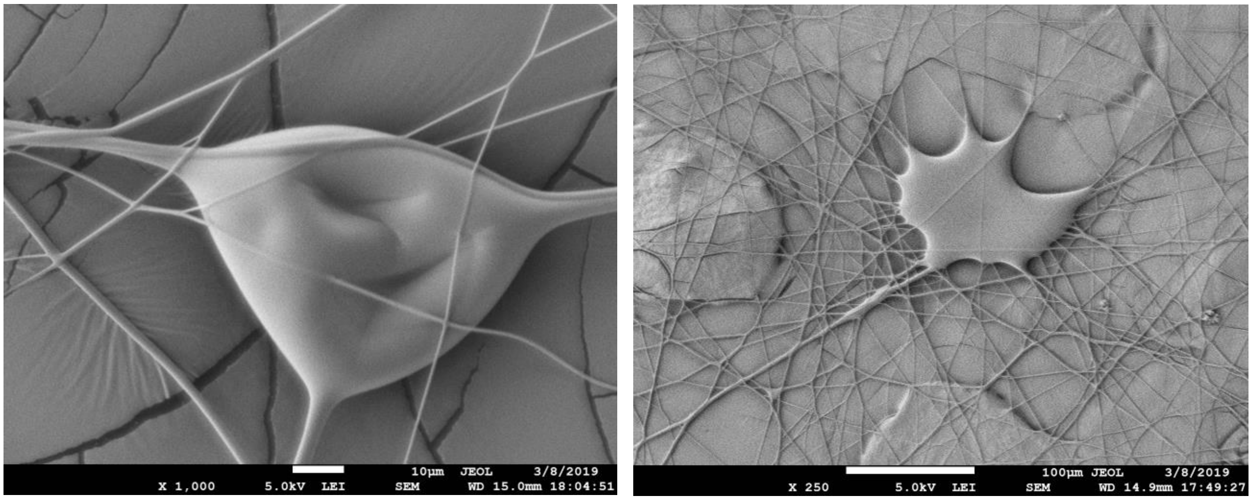

Figure 18. Coagulations of polymer solution can decrease uniformity in network, decrease transparency, and decrease conductance.

CHAPTER IV

CONCLUSION

The fabrication of FTEs can be highly optimized by varying characteristics of the nanofiber networks. To achieve highly conductive, highly transparent, strong, flexible electrodes, nanofibers should be thick, randomly organized, and have large spaces between fibers. These characteristics were achieved by collecting fibers across a 1 inch long copper circular frame collector of 0.75 inch diameter placed on a flat plate. The collection site was 10 cm from the tip of the 30 mm long, 0.6 mm diameter syringe needle. The syringe held an aqueous polymer solution made of 8 wt.% PVP to 92 wt.% solvent, where the solvent was composed of 90 wt.% ethanol and 10 wt.% deionized water. The solution was pushed from the syringe at a rate of 0.6 μL/min. The system was run at 10 kV until the nanofiber network became visible across the collector (between 4 to 7 minutes). Several finished samples are shown in Figure 19.

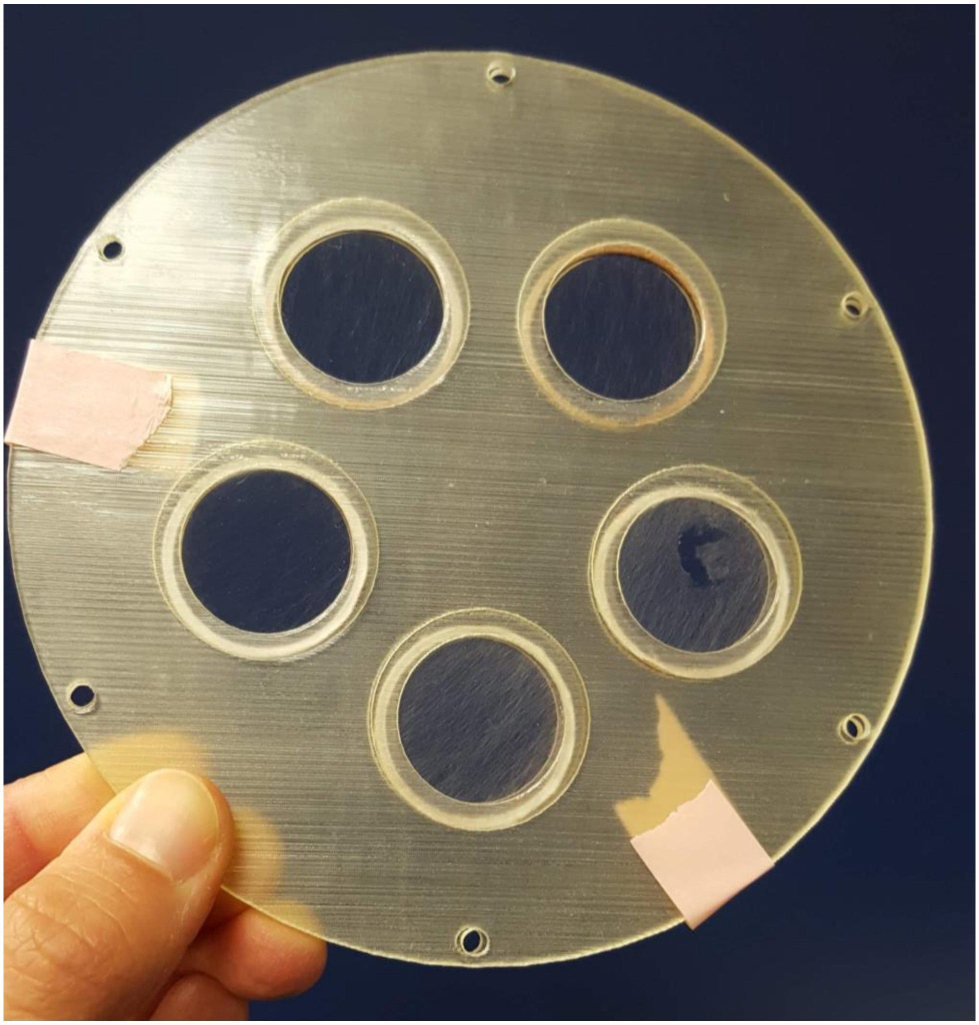

Figure 19. Optimized electrospun nanofiber network samples.

The average nanofiber networks produced by these optimized electrospinning settings had diameters from 600 nm to 3 μm with an average diameter of 1.54 μm. Average spaces between fibers averaged 4393 μm^2 in area.

Future work is needed to test the flexibility, strength, and transparency of these FTEs after copper has been deposited and the polymer fibers dissolved away. Metal oxides that are light in color, such as TiO_2, MgO, and Al_2O_3 are recommended as strong candidates for high-performing protective layers.

REFERENCES

[1] C. F. Guo and Z. Ren, "Flexible transparent conductors based on metal nanowire networks," *Mater. Today*, vol. 18, no. 3, pp. 143–154, Apr. 2015.

[2] B. W. An *et al.*, "Stretchable and Transparent Electrodes using Hybrid Structures of Graphene–Metal Nanotrough Networks with High Performances and Ultimate Uniformity," *Nano Lett.*, vol. 14, no. 11, pp. 6322–6328, Nov. 2014.

[3] H. Wu *et al.*, "A transparent electrode based on a metal nanotrough network," *Nat. Nanotechnol.*, vol. 8, no. 6, pp. 421–425, Jun. 2013.

[4] P. Kou, L. Yang, C. Chang, and S. He, "Improved Flexible Transparent Conductive Electrodes based on Silver Nanowire Networks by a Simple Sunlight Illumination Approach," *Sci. Rep.*, vol. 7, no. 1, p. 42052, Dec. 2017.

[5] Z. Chen, S. Ye, I. E. Stewart, and B. J. Wiley, "Copper Nanowire Networks with Transparent Oxide Shells That Prevent Oxidation without Reducing Transmittance," *ACS Nano*, vol. 8, no. 9, pp. 9673–9679, Sep. 2014.

[6] J. Chen *et al.*, "Solution-processed copper nanowire flexible transparent electrodes with PEDOT:PSS as binder, protector and oxide-layer scavenger for polymer solar cells."

[7] J. Chen *et al.*, "Direct Growth of Flexible Carbon Nanotube Electrodes," *Adv. Mater.*, vol. 20, no. 3, pp. 566–570, Feb. 2008.

[8] †,§ Daihua Zhang *et al.*, "Transparent, Conductive, and Flexible Carbon Nanotube Films and Their Application in Organic Light-Emitting Diodes," 2006.

[9] L. Hu, and D. S. Hecht, and G. Grüner*, "Percolation in Transparent and Conducting Carbon Nanotube Networks," 2004.

[10] M. W. Rowell *et al.*, “Organic solar cells with carbon nanotube network electrodes,” *Appl. Phys. Lett.*, vol. 88, no. 23, p. 233506, Jun. 2006.

[11] S. Bae *et al.*, “Roll-to-roll production of 30-inch graphene films for transparent electrodes,” *Nat. Nanotechnol.*, vol. 5, no. 8, pp. 574–578, Aug. 2010.

[12] J.-U. Park, S. Nam, M.-S. Lee, and C. M. Lieber, “Synthesis of monolithic graphene–graphite integrated electronics,” *Nat. Mater.*, vol. 11, no. 2, pp. 120–125, Feb. 2012.

[13] K. V. Emtsev *et al.*, “Towards wafer-size graphene layers by atmospheric pressure graphitization of silicon carbide,” *Nat. Mater.*, vol. 8, no. 3, pp. 203–207, Mar. 2009.

[14] X. Li *et al.*, “Transfer of Large-Area Graphene Films for High-Performance Transparent Conductive Electrodes,” *Nano Lett.*, vol. 9, no. 12, pp. 4359–4363, Dec. 2009.

[15] K. K. Kim *et al.*, “Enhancing the conductivity of transparent graphene films via doping,” *Nanotechnology*, vol. 21, no. 28, p. 285205, Jul. 2010.

[16] S. De *et al.*, “Silver Nanowire Networks as Flexible, Transparent, Conducting Films: Extremely High DC to Optical Conductivity Ratios,” *ACS Nano*, vol. 3, no. 7, pp. 1767–1774, Jul. 2009.

[17] V. Scardaci, R. Coull, P. E. Lyons, D. Rickard, and J. N. Coleman, “Spray Deposition of Highly Transparent, Low-Resistance Networks of Silver Nanowires over Large Areas,” *Small*, vol. 7, no. 18, pp. 2621–2628, Sep. 2011.

[18] E. C. Garnett *et al.*, “Self-limited plasmonic welding of silver nanowire junctions,” *Nat. Mater.*, vol. 11, no. 3, pp. 241–249, Mar. 2012.

[19] P. E. Lyons *et al.*, “High-Performance Transparent Conductors from Networks of Gold Nanowires,” *J. Phys. Chem. Lett.*, vol. 2, no. 24, pp. 3058–3062, Dec. 2011.

[20] H. Wu *et al.*, “Electrospun Metal Nanofiber Webs as High-Performance Transparent

Electrode," *Nano Lett.*, vol. 10, no. 10, pp. 4242–4248, Oct. 2010.

[21] D.-S. Leem, A. Edwards, M. Faist, J. Nelson, D. D. C. Bradley, and J. C. de Mello, "Efficient Organic Solar Cells with Solution-Processed Silver Nanowire Electrodes," *Adv. Mater.*, vol. 23, no. 38, pp. 4371–4375, Oct. 2011.

[22] M.-G. Kang, M.-S. Kim, J. Kim, and L. J. Guo, "Organic Solar Cells Using Nanoimprinted Transparent Metal Electrodes," *Adv. Mater.*, vol. 20, no. 23, pp. 4408–4413, Dec. 2008.

[23] J. van de Groep, P. Spinelli, and A. Polman, "Transparent Conducting Silver Nanowire Networks," *Nano Lett.*, vol. 12, no. 6, pp. 3138–3144, Jun. 2012.

[24] V. B. Nam and D. Lee, "Copper Nanowires and Their Applications for Flexible, Transparent Conducting Films: A Review.," *Nanomater. (Basel, Switzerland)*, vol. 6, no. 3, Mar. 2016.

[25] K. Kim *et al.*, "All-Solution-Processed Thermally and Chemically Stable Copper–Nickel Core–Shell Nanowire-Based Composite Window Electrodes for Perovskite Solar Cells," *ACS Appl. Mater. Interfaces*, vol. 10, no. 36, pp. 30337–30347, Sep. 2018.

[26] F.-Q. Zhang, Y. Hu, X.-M. Meng, and K.-Q. Peng, "Fabrication and photoelectrochemical properties of silicon/nickel oxide core/shell nanowire arrays," *RSC Adv.*, vol. 5, no. 107, pp. 88209–88213, Oct. 2015.

[27] Y. Ahn, Y. Jeong, D. Lee, and Y. Lee, "Copper Nanowire–Graphene Core–Shell Nanostructure for Highly Stable Transparent Conducting Electrodes," *ACS Nano*, vol. 9, no. 3, pp. 3125–3133, Mar. 2015.

[28] J. S. Bunch *et al.*, "Impermeable Atomic Membranes from Graphene Sheets," *Nano Lett.*, vol. 8, no. 8, pp. 2458–2462, Aug. 2008.

[29] A. A. Balandin *et al.*, "Superior Thermal Conductivity of Single-Layer Graphene," *Nano Lett.*, vol. 8, no. 3, pp. 902–907, Mar. 2008.

[30] "15 Year Copper/Gold Price Ratio Chart," *InfoMine Inc.*, 2019. [Online]. Available: http://www.infomine.com/investment/price-ratios/copper-gold/15-year/. [Accessed: 07-Apr-2019].

[31] J.-S. Park, "Electrospinning and its applications," *Adv. Nat. Sci. Nanosci. Nanotechnol.*, vol. 1, no. 4, p. 43002, 2010.

[32] M. K. Leach, Z.-Q. Feng, S. J. Tuck, and J. M. Corey, "Electrospinning Fundamentals: Optimizing Solution and Apparatus Parameters," *J. Vis. Exp.*, no. 47, pp. e2494–e2494, Jan. 2011.

[33] W.-E. Teo, "Electrospinning Cheat Sheet," *ElectrospinTech*, 2015. [Online]. Available: http://electrospintech.com/espinmemcheatsheet.html#.XKtPQJhKg2w. [Accessed: 08-Apr-2019].

[34] "Scanning Electron Microscopy - Nanoscience Instruments," *Nanoscience Instruments*. [Online]. Available: https://www.nanoscience.com/techniques/scanning-electron-microscopy/. [Accessed: 08-Apr-2019].

[35] "Sputtering Technology, Physical Vapor Deposition," *Angstrom Sciences*. [Online]. Available: https://www.angstromsciences.com/sputtering-technology. [Accessed: 09-Nov-2018].

[36] N. Hardy, "Thin Film Deposition By Sputtering: Essential Basics," *Semicore Equipment, Inc.*, 2013. [Online]. Available: http://www.semicore.com/news/70-thin-film-deposition-sputtering. [Accessed: 09-Nov-2018].